

SCIENTIFIC REPORTS



OPEN

The TRPM1 channel in ON-bipolar cells is gated by both the α and the $\beta\gamma$ subunits of the G-protein G_o

Ying Xu^{1,5}, Cesare Orlandi², Yan Cao², Shengyan Yang¹, Chan-Il Choi³, Vijayakanth Pagadala³, Lutz Birnbaumer³, Kirill A. Martemyanov² & Noga Vardi⁴

Received: 30 September 2015

Accepted: 16 December 2015

Published: 17 February 2016

Transmission from photoreceptors to ON bipolar cells in mammalian retina is mediated by a sign-inverting cascade. Upon binding glutamate, the metabotropic glutamate receptor mGluR6 activates the heterotrimeric G-protein $G_{\alpha_o}\beta_3\gamma_{13}$, and this leads to closure of the TRPM1 channel (melastatin). TRPM1 is thought to be constitutively open, but the mechanism that leads to its closure is unclear. We investigated this question in mouse rod bipolar cells by dialyzing reagents that modify the activity of either G_{α_o} or $G\beta\gamma$ and then observing their effects on the basal holding current. After opening the TRPM1 channels with light, a constitutively active mutant of G_{α_o} closed the channel, but wild-type G_{α_o} did not. After closing the channels by dark adaptation, phosducin or inactive G_{α_o} (both sequester $G\beta\gamma$) opened the channel while the active mutant of G_{α_o} did not. Co-immunoprecipitation showed that TRPM1 interacts with $G\beta_3$ and with the active and inactive forms of G_{α_o} . Furthermore, bioluminescent energy transfer assays indicated that while G_{α_o} interacts with both the N- and the C- termini of TRPM1, $G\beta\gamma$ interacts only with the N-terminus. Our physiological and biochemical results suggest that both G_{α_o} and $G\beta\gamma$ bind TRPM1 channels and cooperate to close them.

In mammalian retina, an increase in light intensity hyperpolarizes the photoreceptor and initiates two opposing signals: sign-preserving synaptic transmission to the OFF bipolar cells and sign-inverting transmission to the ON bipolar cells. In darkness, the depolarized photoreceptors tonically release glutamate into the synaptic cleft, hyperpolarizing the ON bipolar cells. Light hyperpolarizes the photoreceptors, reducing glutamate in the cleft and causing the ON bipolar cells to depolarize. The key steps in this 'sign inverting' cascade are: glutamate activates the ON bipolar cell's mGluR6 receptor^{1–3}, and this activates the heterotrimeric G-protein G_o that comprises $\alpha_o\beta_3\gamma_{13}$ ^{4–10}. Active G_o closes the non-selective cation channel TRPM1 (melastatin), thought to be constitutively active^{11–14}. In the retina, TRPM1 is required for night vision as mutations in its gene or autoimmune targeting of the protein lead to lack of the ERG b-wave and to night blindness^{15–18}. Outside the retina, two splice variants of TRPM1 regulate pigmentation in melanocytes, and loss of this gene is correlated with tumor aggressiveness in human melanoma^{19–21}.

While there is strong evidence that active G_o closes the TRPM1 channel, it is not clear if this closure is caused by an active G_{α_o} , or a free $G\beta\gamma$ dimer. Evidence indicating that G_{α_o} induces this closure is based on studies that transfected TRPM1 into CHO cells and found that applying activated G_{α_o} purified from the brain to an excised patch closed the channel, but applying $G\beta\gamma$ did not. These studies also found that co-transfecting CHO cells with TRPM1 and constitutively active G_{α_o} rendered the TRPM1 channels inactive¹². Evidence indicating that $G\beta\gamma$ causes TRPM1 closure is based on results from several cell types, including bipolar cells, where dialyzing $G\beta\gamma$ reduced the mGluR6-initiated response, but dialyzing an activated form of G_{α_o} did not. Further support comes from transfected HEK cells and human melanocytes where $G\beta\gamma$ rather than active G_{α_o} reduced a Ca^{2+} signal triggered with high extracellular Ca^{2+} ²². These contradicting data could result from the use of different cell lines that express different endogenous molecules that impact the channel. Indeed, activating endogenous mGluR6 in melanocytes opens the channel instead of closing it; but after expressing G_{α_o} by transfection, mGluR6 activation

¹GHM Institute of CNS Regeneration, Jinan University, Guangzhou, 510632, China. ²Department of Neuroscience, The Scripps Research Institute, Jupiter, FL 33458, USA. ³National Institute of Environmental Health Sciences., Research Triangle Park, NC 27709, USA. ⁴Department of Neuroscience, University of Pennsylvania, Philadelphia, PA 19104, USA. ⁵Co-Innovation Center of Neuroregeneration, Nantong University, Jiangsu, China. Correspondence and requests for materials should be addressed to Y.X. (email: xuying@jnu.edu.cn) or N.V. (email: noga@mail.med.upenn.edu)

closes the channel²³. To better understand how the TRPM1 channel operates in retinal ON bipolar cells, we carried out a battery of experiments in which we dialyzed reagents that modify the status of the endogenous G-protein in rod bipolar cells and observed their effects on the basal current and on the light response. We further examined the interaction of G-protein subunits with TRPM1 using co-immunoprecipitation and energy transfer assays. Our results suggest that both $G\alpha_o$ and $G\beta\gamma$ bind the TRPM1 channels and together cooperate to close them.

Results

Our experiments involved blocking K^+ and Cl^- channels, then dialyzing reagents into rod bipolar cells clamped at -60 mV, and then testing over time the reagents' effects on the holding inward current. Given that most channels are blocked and only TRPM1 is likely to be gated by G_o , the change in holding current indicates whether the TRPM1 channels are opening or closing in response to the dialyzed agent. We chose to monitor the holding current as the read out of the reagents' effects rather than the size of the mGluR6-initiated response (as done by Shen *et al.*) because the mGluR6 response is likely to decrease regardless of whether channels are opened or closed by the reagent.

In light-exposed retinas, dialyzing active $G\alpha_o$ closes the TRPM1 channel. In order to test if $G\alpha_o$ closes the channel, we had to first open the channels. Therefore, as soon as we established a seal, we provided a light step and then tested if the dialyzed solution closed the channel (see example in Fig. 1A). Every 35 sec we provided a voltage ramp to test slope conductance, and then briefly turned off the light to monitor OFF responses. Each of these 35-sec-protocol repetitions is referred to as a sweep, and a typical experiment had 5 sweeps. In general, the light step produced a large transient increase of the inward current followed by a smaller sustained current (Fig. 1A). Because our experiments required recording periods longer than the diffusion time (time scale of sec), and because BAPTA does not prevent the adapting fall off of the light response (as it only affects the response in the msec range), it was necessary to compare the sustained current that was achieved 13 sec after break-in. To compare this light-evoked sustained current before and after dialysis, we averaged the currents over 0.5 sec at the 1st and 5th sweeps (Fig. 1B). To determine if the dialyzed solution caused a statistically significant change, we applied the paired Students t-test. This test computes the probability that the average difference between the two time points is equal to 0 (i.e., it computes the probability that the dialyzed agent has no effect). We also provided voltage ramps to monitor changes in the slope conductance; this was computed in the linear range between -95 mV and -65 mV (to avoid contributions from the voltage-activated L-type calcium channel) (Fig. 1C). In control experiments (with only basic pipette solution), the inward sustained current remained relatively stable at around -34 pA ($n = 14$ cells; Table 1). Then, to test our method, we confirmed established observations that dialyzing $GTP\gamma S$ closes TRPM1^{24,25}. When $50\ \mu M$ $GTP\gamma S$ was perfused, only 5 out of 13 cells gave a light response. Since cells without responses could not be tested for channel closure, we increased the yield by switching to $25\ \mu M$ $GTP\gamma S$ which evoked light responses in 6 out of 7 cells. Combining results from both concentrations, we found that the sustained current started at -37.3 ± 7.1 pA, and as expected, greatly decreased during dialysis. At the 5th time point, the holding sustained current was -16.1 ± 4.1 pA, significantly lower than that at the 1st time point ($p < 0.01$ paired Student's t-test; Table 1). This indicates that $GTP\gamma S$ closes the channels that were opened by light. To illustrate the net effect of each dialyzed agent, we plotted the average difference in the sustained currents between the 5th and the 1st time points. Positive values indicate channel closure because the inward current becomes less negative (Fig. 1D).

Next we tested the effect of dialyzing a constitutively active mutant of $G\alpha_o$. Previous experiments testing this effect activated the $G\alpha_o$ subunit with $GTP\gamma S$ or with $GMP\text{-}P(NH)P^{12,14,22}$. These approaches may have led to an excess of the non-hydrolysable GTP analogue in the solution, making it unclear whether the observed effect was caused only by active $G\alpha_o$ or also by activation of $G\beta\gamma$. Therefore we took the approach of producing a constitutively active mutant of myristoylated $G\alpha_o$ (myr $G\alpha_o$ -QL) and incubating it with GTP prior to introducing it into the cells. This QL mutation prevents GTP from being hydrolyzed, thus profoundly shifting its conformation to the active state in the presence of GTP^{26,27}. We found that after dialyzing 40 nM of myr $G\alpha_o$ -QL (with GTP as in the control solution), the light-evoked sustained current significantly dropped from -34.3 ± 6.3 to -26.1 ± 4.4 pA ($n = 17$, $p = 0.029$) (Fig. 1D and Table 1).

We then dialyzed wild type myristoylated $G\alpha_o$ (100 nM), also after incubating it with GTP. Unlike the QL mutant, WT myr $G\alpha_o$ hydrolyzes all bound GTP within about 1–2 minutes²⁸ and hence is expected to be largely inactive in its GDP-bound form when delivered into the cells. For WT myr $G\alpha_o$, the sustained current remained stable throughout the experiment (ranging between -29 pA and -31 pA; $n = 17$), as it did with the control solution (Fig. 1D). If a decrease in sustained current indicates that channels are closing, these current changes should correlate with changes in the slope conductance. Indeed, increases in sustained current were highly correlated with increases in slope conductance ($R = -0.92$; the minus sign results from inward currents being assigned negative values).

To confirm that these conductance changes were due to TRPM1 modulation, in several experiments we extended the light OFF period to 4 sec and provided a voltage ramp during this period. We then subtracted for each sweep the I-V curve during light OFF from that during light ON, thus isolating the contribution of TRPM1 to the measured current at different voltages. At the first sweep, TRPM1 contribution was significant (supp. Fig. 1), but at the 5th sweep it was practically null, indicating that TRPM1 was closed and that the main difference seen during light ON was due to TRPM1. Thus we conclude that the closure of TRPM1 observed when dialyzing myr $G\alpha_o$ -QL is due to $G\alpha_o$'s active state. While we cannot compare the effect of $G\alpha_o$ -QL to that of $GTP\gamma S$ because of the difference in concentrations, diffusion properties, and nature of the activity, it appears that the effect of

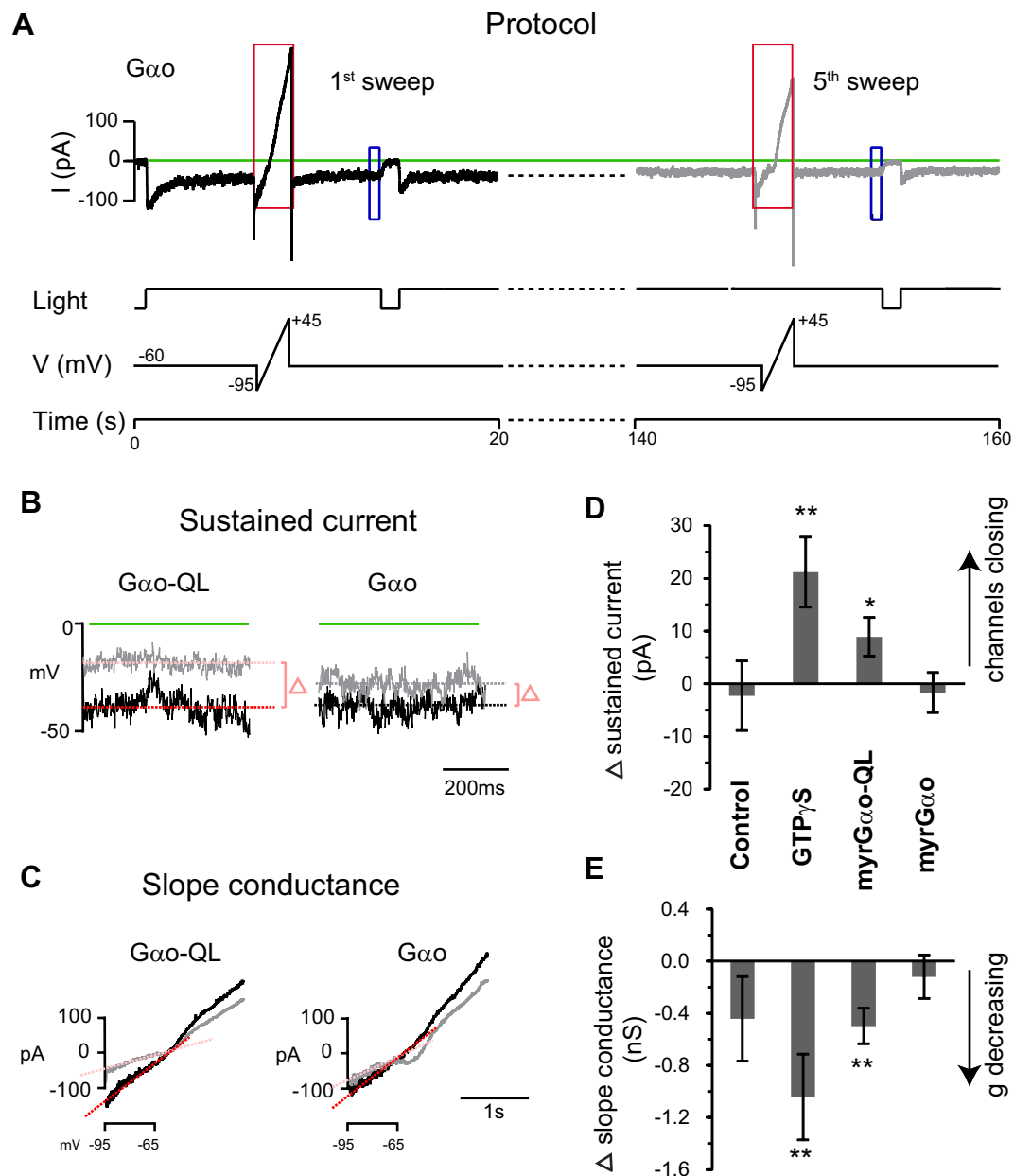


Figure 1. GTP γ S and active myrG α_o close the TRPM1 channel (under light adaptation). (A) The protocol for light adapted conditions (illustrated with a record from a cell dialyzed with myr-G α_o): Immediately after break-in, cells were clamped at -60 mV, and then after 0.5 sec, a background light of 1.1×10^4 photons $\mu\text{m}^{-2} \text{s}^{-1}$ was applied; 6.5 s after break-in (and every 35 s thereafter), a 2 s voltage ramp from -95 mV to $+45$ mV was applied, and 13.5 s after break-in (and every 35 s thereafter), the light was turned off for 1 s (or occasionally for 4 s). Dotted lines between the 1st (black) and 5th (gray) sweeps indicate continued recordings. The initial light ON stimulus elicited a strong inward current that decayed due to adaptation. Blue and red boxes indicate the traces that are expanded in (B,C). (B) The sustained inward current under light was measured by averaging the currents over 0.5 sec before light OFF (indicated by blue rectangular boxes). The average inward current at the 1st sweep (black trace) is drawn as a red line, and that at the 5th (gray) is pink. The difference is indicated by the delta symbol. (C) Slope conductance was computed from the current responses to voltage ramp (shown in red boxes in A) between -95 mV to -65 mV (the linear range). The computed slopes are color coded as in (B). (D) Average differences in the sustained holding currents under light for four dialyzed solutions: control (normal pipette solution), 25 or 50 μM GTP γ S, 40 nM constitutively active myrG α_o -QL, or 100 nM WT myrG α_o . When current doesn't change, the difference is 0; when channels are closing, the inward current is less negative and the difference is positive. (E) Change in slope conductance for the same four solutions in (D). When the slope conductance decreases, the difference is negative. *indicates a significant difference ($p < 0.05$) between the 1st and 5th time points, and **indicates a highly significant difference ($p < 0.01$).

	Control	GTP γ S	myrG α_o	myrG α_o -QL
I (1 st) \pm SEM	-33.80 \pm 8.25	-37.27 \pm 7.09	-29.25 \pm 4.91	-34.31 \pm 6.26
P (reagent vs control at 1 st)		0.77	0.64	0.96
I (5 th) \pm SEM	-36.07 \pm 6.51	-16.07 \pm 4.10	-30.92 \pm 4.11	-26.15 \pm 4.37
P (reagent vs control at 5 th)		0.03	0.51	0.21
P (paired Student t-test)	0.74	0.009	0.67	0.029

Table 1. Summary of light-evoked sustained currents under different dialyzed solutions. The first row shows the light-evoked sustained currents (I) \pm SEM for the first time point; the second row shows the P values obtained with Student's t-test when comparing the data for each reagent at the 1st time point to that of control at the 1st time point. The third row shows the currents (I) \pm SEM for the 5th data point and the fourth row shows the P value obtained with Student's t-test when comparing the data for each reagent at the 5th time point to that of control at the 5th time point. The last row shows the P values obtained with paired student t-test comparing 1st to 5th time points for each reagent.

active myrG α_o is smaller than that of GTP γ S. If so, this smaller effect may be due to an additional effect by G $\beta\gamma$ (which is also activated by GTP γ S).

Sequestering G $\beta\gamma$ opens the TRPM1 channel in the dark. To test the effect of G $\beta\gamma$ on TRPM1, Shen *et al.* dialyzed recombinant G $\beta 1\gamma 2$ or native G $\beta\gamma$ subunits purified from the brain into rod bipolar cells²². They found that G $\beta\gamma$ reduced responses to light and to mGluR6 antagonists, suggesting that G $\beta\gamma$ closes the channel and prevents it from opening. In apparent disagreement, applying G $\beta\gamma$ to an inside-out excised patch of TRPM1-transfected CHO cells did not change the probability of channel opening¹². To address these opposite findings, we tested the contribution of G $\beta\gamma$ in rod bipolar cells using the approach of inhibiting the endogenous G $\beta\gamma$ by sequestering it with G α_o -GDP or phosducin, a 28 kDa phospho-protein that binds G $\beta\gamma$ and thus inhibits activity of the free dimer^{29–32}. These experiments were performed on dark-adapted cells to induce a state in which G $\beta\gamma$ is dissociated from the endogenous G α_o . The cells were clamped at -60 mV, and the dark holding current (which we term basal current) was measured at different time points after break-in (see example in Fig. 2A). Every 35 sec during the recording period, we provided a voltage ramp in darkness to test slope conductance followed by a strong 10 msec light flash to test the cell's ability to produce a light response (Fig. 2A). For cells that were patched with control solution in the pipette, the average basal current at the first time point (10 sec after break-in) was -25.8 \pm 4.1 pA, and that at the 5th time point (150 sec after break-in) was -32.0 \pm 3.2 pA ($p = 0.06$, $n = 43$ total over all dark experiments) (Fig. 2D and Table 2), indicating relative stability in the holding current.

Next, we dialyzed myrG α_o at both 40 nM and 100 nM concentrations. This increased the basal inward current in a concentration-dependent manner. While 40 nM myrG α_o increased the basal current at the 5th time point by a factor of 1.22 (from -49.2 \pm 7.5 pA to -60.1 \pm 9.5 pA; $n = 12$; $p = 0.4$), 100 nM myrG α_o increased it by a factor of 2 (from -27.6 \pm 3.6 pA to -54.4 \pm 6.4 pA; $n = 24$; $p < 0.01$) (Fig. 2B,D). To determine if this increase in basal current is due to G α_o -GDP or if it would happen independent of G α_o 's nucleotide-bound state, we dialyzed myrG α_o -QL (40 nM) and found it did not cause any change in basal current (37.2 \pm 5.5 pA and -32.9 \pm 4.1 pA for 1st and 5th time points, respectively; $n = 22$; $p = 0.30$) (Table 2 and Fig. 2D). We wondered if longer dialysis would make a difference, so for some experiments we measured the current at the 10th time point. For myrG α_o -QL, the holding current remained similar (from -38.4 \pm 6.6 to -37.7 \pm 5.3 pA; $n = 16$; $p = 0.88$) (sup Fig. 2), but for 40 nM WT myrG α_o , the current continued to increase (-67.4 \pm 10.9 at the 10th time point; $p = 0.03$) (supp Fig. 2). These findings indicate that the opening of the TRPM1 channels by wild type G α_o is due to its GDP-bound state.

Next, we tested the effect of dialyzing phosducin, a reagent that offers the advantage of preventing G $\beta\gamma$ from interacting with effectors without affecting the activation state of G α and without changing its concentration³³. When 9 μ M phosducin was added to the pipette solution, the basal inward current progressively increased from -29.9 \pm 5.9 pA to -45.3 \pm 7.3 pA; $n = 14$; $p = 0.01$) (Fig. 2D). This change in basal current highly correlated with the change in slope conductance: while this conductance decreased a little for control and myrG α_o -QL, it increased for both WT myrG α_o and phosducin. The correlation between basal current and slope conductance was -0.91 (Fig. 2C,E), supporting the notion that an increase in basal current indicates channel opening. Thus, our results show that dialyzing reagents that sequester G $\beta\gamma$ opens TRPM1 channels, suggesting that G $\beta\gamma$ closes the channel.

Linoleic and myristic acids do not modulate TRPM1. In the experiments above, we used myristoylated forms of G α_o because native G α_o harbors this post-translational modification that is important for its normal association with the membrane³⁴. However, because lipids are well known to mediate or modulate gating of TRP channels^{35–37}, we tested if the myristoyl group present on myrG α_o may contribute directly to channel opening in our experiments by using non-myristoylated G α_o where the myristoylation signal at the N-terminus was replaced with a His₆ affinity tag (His-G α_o). Similar to myrG α_o , 150 or 300 nM His₆-G α_o increased the basal inward current (from -7.9 \pm 2.7 pA to -28.7 \pm 7.0 pA; $n = 9$; $p = 0.013$) as well as the slope conductance (Fig. 2D,E).

Next, since puffing certain lipid modifiers on the extracellular face of the plasma membrane can modulate certain TRP channels^{38–40}, we further tested TRPM1 modulation by puffing alpha linoleic acid (LNA, 20–100 μ M; 5 cells) or myristic acid (MA, 100–250 μ M; 8 cells). We found that although these cells responded to light, they

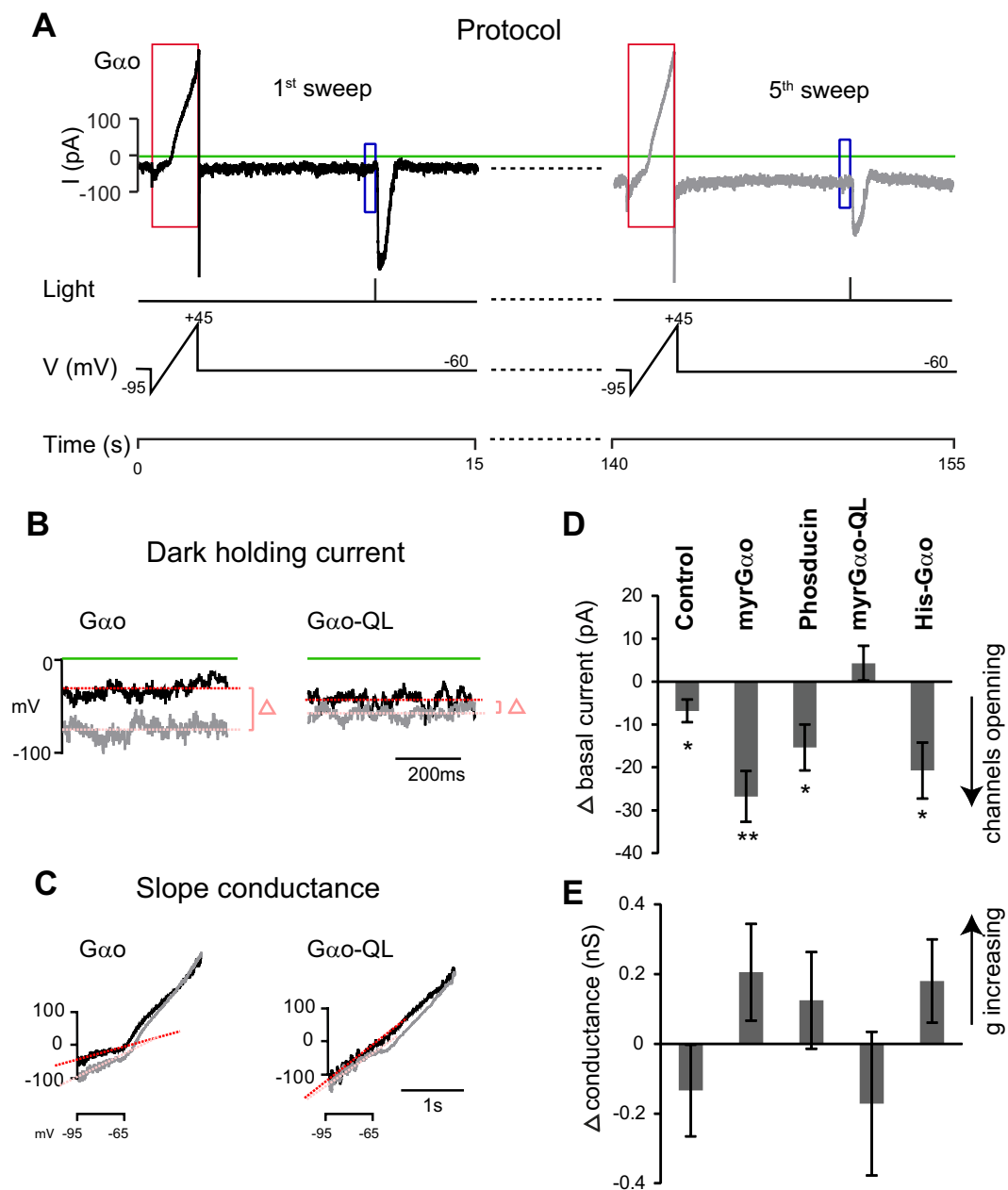


Figure 2. Sequestering $G\beta\gamma$ opens the TRPM1 channel (under dark adaptation). (A) The protocol of a dark adapted experiment (illustrated with a record from a cell dialyzed with myr- $G\alpha_o$): 0.5 sec after break-in, a 2 s voltage ramp was applied, and 10.5 sec after break-in, a 50 msec light (3.8×10^4 photons $\mu\text{m}^{-2} \text{s}^{-1}$) was flashed. This cycle was repeated every 35 s. The 1st sweep is shown in black, the 5th sweep in gray. (B) The dark inward current was measured by averaging the currents over 0.5 sec before the light flash (indicated by blue rectangular boxes in A). Black trace is from the 1st sweep, gray is from the 5th. The average holding current at the 1st sweep is indicated by a red line, and that at the 5th by a pink line. The difference is indicated by the delta symbol on the right. (C) Slope conductance was computed from the current responses to the voltage ramp (shown in red boxes in A) between -95 mV to -65 mV (the linear range). First ramp is in black, 5th in gray. The slopes for these records are shown in red and pink, correspondingly. (D) Quantitative analysis of changes in the dark holding currents for five different conditions: control, 100 nM myr $G\alpha_o$, 9 μM phosducin, 40 nM myr $G\alpha_o$ -QL, and 150–300 nM His- $G\alpha_o$. When channels are opening, the inward current increases (has a more negative value) and the difference between the 5th and the 1st time points is negative. (E) Quantitative analysis of changes in slope conductance for each of the above conditions. *indicates a significant difference ($p < 0.05$) between the 1st and 5th time points, and **indicates a highly significant difference ($p < 0.01$).

	Control	myrG α o	His G α o	phosducin	myrG α o-QL
I (1 st) \pm SEM	-25.8 \pm 4.1	-27.6 \pm 3.6	-7.9 \pm 2.7	-29.9 \pm 5.9	-37.2 \pm 5.5
P (reagent vs control at 1 st)		0.765	0.054	0.595	0.103
I (5 th) \pm SEM	-32.0 \pm 3.2	-54.4 \pm 6.4	-28.7 \pm 7.0	-45.3 \pm 7.3	-32.9 \pm 4.1
P (reagent vs control at 5 th)		0.0009	0.668	0.061	0.861
P (paired Student t-test)	0.062	0.0002	0.013	0.013	0.301

Table 2. Summary of basal currents in the dark under different dialyzed solutions. For explanation refer to Table 1, except that here we present the basal current under dark.

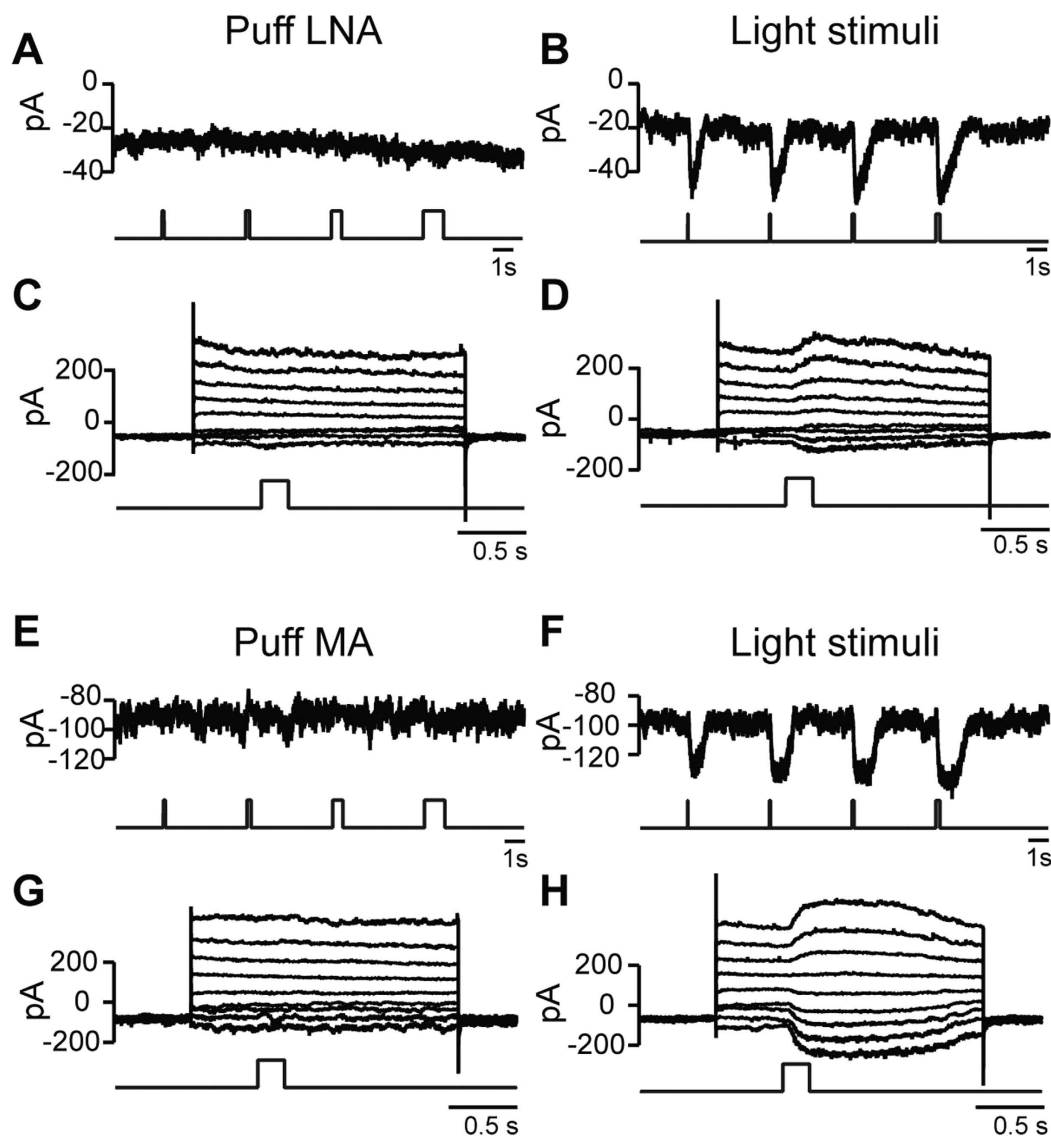


Figure 3. Alpha linoleic acid and myristic acid do not modulate the channel. (A) An example of a cell clamped at -60 mV and puffed with $100 \mu\text{M}$ alpha linoleic acid (LNA) of different puff durations indicated by the lower trace. (B) Same cell stimulated with light for different durations. (C,D) Same cell clamped at different voltages from -95 mV to $+65$ mV with 20 mV steps and either puffed with LNA for 0.2 sec (C) or flashed for 0.2 sec (D). The cell responds to light, but not to LNA. (E–H) As for (A–D), but puffed with $100 \mu\text{M}$ myristic acid (MA). Again, no response to the myristic acid was observed.

did not respond to the lipid modifiers (Fig. 3), indicating that the main mechanism for channel opening is solely through the G-protein.

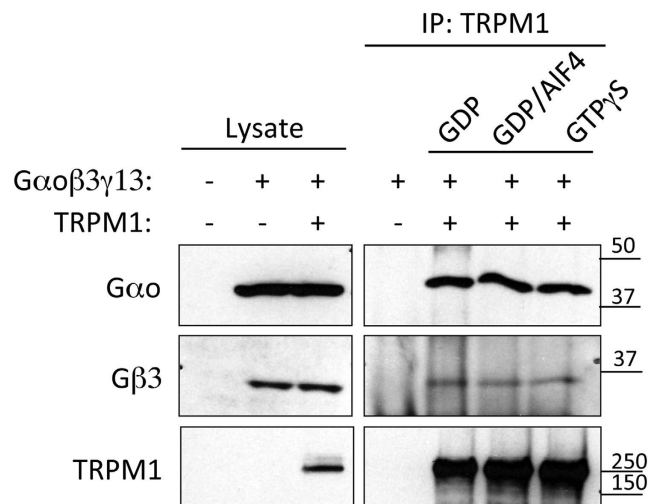


Figure 4. $G\alpha_o$ and $G\beta_3\gamma_{13}$ co-immunoprecipitate with TRPM1. Interaction between TRPM1 and G-protein subunits was studied upon co-transfection into HEK293T cells. Cells were lysed and TRPM1 was precipitated by specific antibodies against TRPM1. Proteins present in the lysates and IP eluates were detected by Western blotting. Approximately 6-fold more material was loaded for the eluates relative to the amount of material present in the lysates. Quantification of protein content revealed 70–100% IP efficiency for TRPM1, 10–12% for $G\alpha_o$, and 7–14% for $G\beta_3$ across samples with no significant differences between nucleotide states. The shown Western blots were cropped at the expected molecular weight; both $G\alpha_o$ and $G\beta_3\gamma_{13}$ were precipitated regardless of added nucleotides.

The TRPM1 channel stably associates with both $G\alpha_o$ and $G\beta_3\gamma_{13}$. Our functional experiments suggest that both $G\alpha$ and $G\beta\gamma$ subunits of G_o regulate the TRPM1 channel open state. To support this model with biochemical evidence and to determine if the effect is direct, we examined the interaction of the G-protein subunits with the TRPM1 channel. First, we co-expressed TRPM1 in HEK293T cells with $G\alpha_o$ and the ON bipolar-specific $G\beta\gamma$ combination $G\beta_3\gamma_{13}$. Following cell lysis, TRPM1 was immunoprecipitated and examined for its ability to pull-down $G\alpha_o$ under three conditions: (1) in $G\alpha_o$'s basal state when the lysates were incubated with GDP; (2) in $G\alpha_o$'s transition state induced by AlF₄; and (3) in $G\alpha_o$'s activated state in the presence of GTP γ S. We found that anti-TRPM1 effectively co-immunoprecipitated $G\alpha_o$ as well as $G\beta_3\gamma_{13}$ (3 experiments; Fig. 4). This binding was equivalent across all conditions, suggesting that the association of TRPM1 with $G\alpha_o$ is independent of the activity state of $G\alpha_o$. No binding was observed in the absence of TRPM1, indicating that this interaction is specific.

We further studied the association of G_o subunits with the TRPM1 channel using a Bioluminescence Resonance Energy Transfer (BRET) assay. In this approach, cytoplasmic N-terminal and C-terminal domains of TRPM1 were fused with a highly efficient energy donor (Nluc) and paired with the $G\beta\gamma$ or $G\alpha_o$ subunits fused with Venus, the fluorescent acceptor (Fig. 5A,B). In these experiments we used a prototypic $G\beta\gamma$ pair, $G\beta_1\gamma_2$, for its functional equivalence and effectiveness in gating the TRPM1 Channel²². To direct the TRPM1 fragments to the plasma membrane where the G-protein subunits are naturally found, the constructs were further appended with an engineered membrane localization sequence. When $G\beta\gamma$ was co-transfected with the N-terminus of TRPM1, the acceptor/donor titration experiments revealed a hyperbolic profile of the BRET signal that saturated at an acceptor/donor ratio of about 1 (Fig. 5C). In contrast, when $G\beta_1\gamma_2$ was combined with the C-terminus of TRPM1, the BRET signal was not different from the shallow linear signal observed with membrane-targeted Nluc luciferase (Fig. 5C,D). This suggests that under our experimental conditions only the N-terminus of TRPM1 specifically interacts with $G\beta\gamma$.

When $G\alpha_o$ was used as an energy acceptor, both the N-terminus and the C-terminus fragments produced significant BRET signals, but the N-terminus gave a stronger signal (Fig. 5E,F). These results indicate that both $G\alpha_o$ and $G\beta\gamma$ interact with the TRPM1 channel, and they further localize the site of interaction: while $G\alpha_o$ interacts with both ends of TRPM1, $G\beta\gamma$ appears to interact only with the N-terminus.

Discussion

We present evidence that both $G\alpha_o$ and free $G\beta\gamma$ play a role in modulating the TRPM1 channel open-state. Furthermore, the close association of these subunits with TRPM1 suggests that the actions of the G-protein subunits are direct rather than acting via a second messenger. To our knowledge, this is the first example of a TRP channel that is directly gated by both arms of a G-protein. TRPC4 has been shown to interact with $G\alpha_{12}$, but not with $G\beta\gamma$ ⁴¹.

Role of $G\alpha_o$. The critical piece of evidence that supports the role of $G\alpha_o$ is our finding that dialyzing a constitutively active mutant of this subunit during light exposure leads to channel closure. Under a prolonged strong light stimulus, the majority of the G-protein must be in its inactive form where $G\beta\gamma$ is bound to $G\alpha_o$ -GDP.

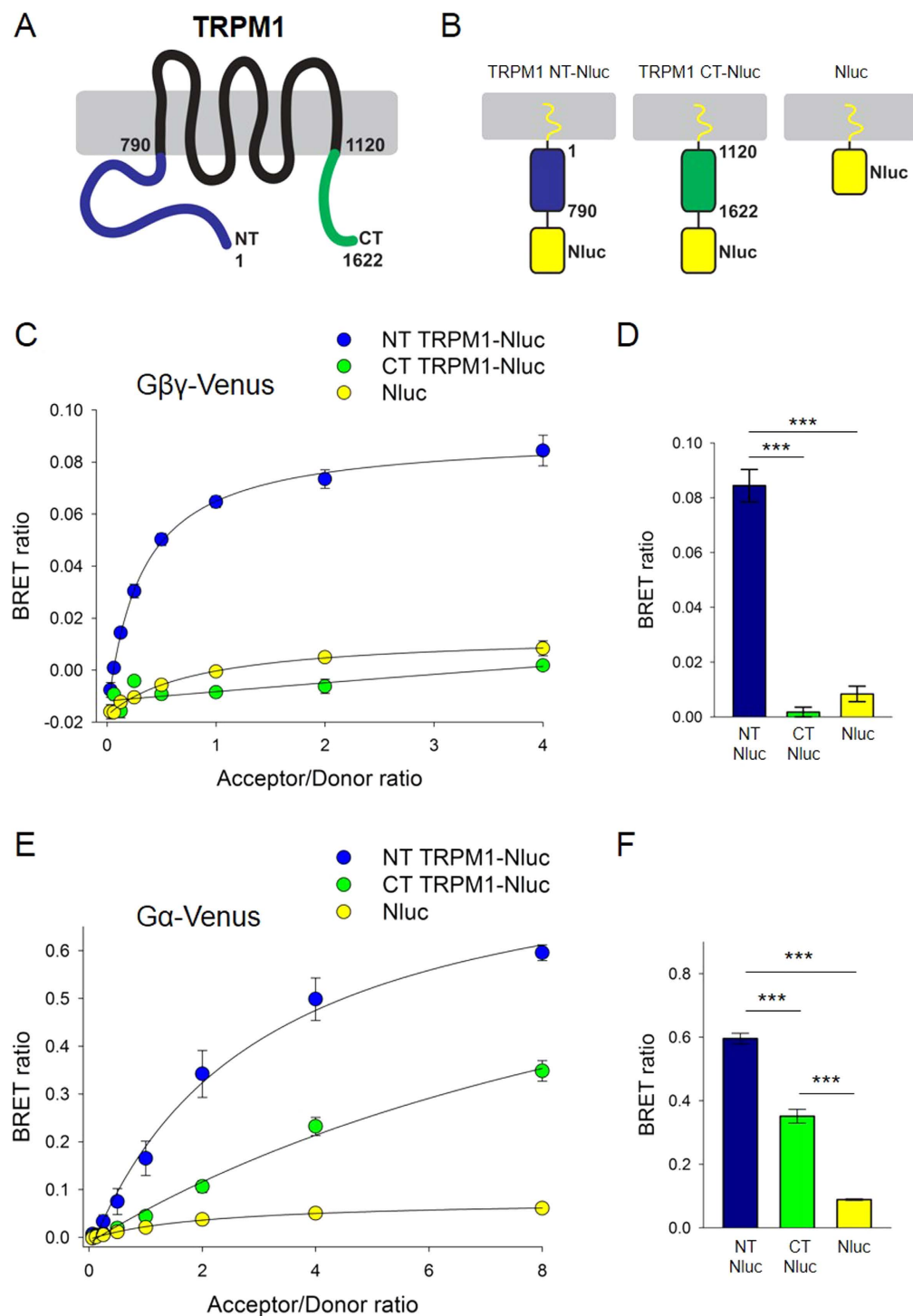


Figure 5. BRET analysis shows interaction between TRPM1-NT and TRPM1-CT with $G\alpha_o$ and $G\beta_1\gamma_2$. HEK293T cells were transfected with fixed amounts of cDNAs coding for TRPM1-derived proteins fused to Nanoluc (donor) and increasing concentrations of cDNAs coding for $G\alpha_o$ or $G\beta_1\gamma_2$ fused to Venus (acceptor). (A) Scheme of TRPM1 with amino acid references of N-terminus (blue) and C-terminus (green). (B) Schemes of the TRPM1-derived constructs used as donors. Each construct had a membrane localization signal at the N-terminus (yellow squiggle) and Nanoluc (Nluc) at the C-terminus. (C) BRET titration assays were performed by measuring energy transfer with increasing concentrations of $G\beta_1\gamma_2$ -Venus and fixed amounts of TRPM1-NT-Nluc or TRPM1-CT-Nluc (mean \pm S.E.; $n = 3$ experiments from 3 different transfections). (D) Quantification and statistical analyses of the BRET assay reported in panel C at the saturating condition of 4:1 acceptor/donor ratio (mean \pm S.E.; $n = 3$; $***p < 0.001$; one way ANOVA followed by Bonferroni post-hoc test). (E) BRET titration assays with increasing concentrations of $G\alpha_o$ -Venus and fixed amounts of TRPM1-NT-Nluc or TRPM1-CT-Nluc (mean \pm S.E.; $n = 3$). (F) Quantification and statistical analyses of the BRET assay reported in panel E at the 8:1 acceptor/donor ratio (mean \pm S.E.; $n = 3$; $***p < 0.001$; one way ANOVA followed by Bonferroni post-hoc test).

Because the dialyzed G_{α_o} -QL does not affect $G\beta\gamma$, the observed channel closure is attributed to the dialyzed reagent and not to $G\beta\gamma$. Since dialyzing wild type G_{α_o} did not change the channel open-state, we conclude that G_{α_o} -GTP contributes to channel closure. This conclusion agrees with experiments showing that application of GMP-P(NH)P-activated G_{α_o} to an excised patch of TRPM1-transfected CHO cells closes the channel, and that transfection with G_{α_o} Q205L renders the channel closed¹⁴. The idea that active G_{α_o} contributes to channel modulation is further supported by our findings that in HEK cells, G_{α_o} -GTP physically associates with TRPM1. Based on these experiments and the excise patch experiment¹⁴, we suggest that the action of G_{α_o} is direct.

TRPM1 open-state requires associated proteins. TRPM1 is thought to be constitutively open because in ON bipolar cells its closure requires activation of G_o . If so, in situations when G_o is naturally inactive, such as in rod bipolar cells lacking mGluR6, TRPM1 channels are expected to stay open. Contrary to this expectation, we previously found that the resting membrane potential in rod bipolar cells lacking mGluR6 is more hyperpolarized than in WT cells by about -15 mV, and the holding current is similar to that of TRPM1-KO^{14,42}. This suggests that TRPM1 requires additional components to stay open. This requirement for an associated protein has also been proposed in two other studies. In the first, it was suggested because TRPM1 was shown to lack 4-fold symmetry⁴³, characteristic of channel oligomerization seen for TRPV1 and other TRP channels, and in the second because capsaicin could not stimulate heterogeneously expressed TRPM1⁴⁴. One possibility is that G_{α_o} is this auxiliary protein, and four lines of evidence support this idea. (1) In melanocytes, which natively do not express G_{α_o} , TRPM1 appears to be constitutively closed and stimulation of mGluR6 opens the channel. When the cells are transfected with G_{α_o} , activation of mGluR6 closes the channel²³. (2) In rod bipolar cells lacking $G_{\alpha_{i/o}}$, TRPM1 seems closed⁸ even though the channel is expressed in the dendritic tips as in WT cells, and $G\beta\gamma$ is practically absent⁴⁵. (3) G_{α_o} -GDP interacts with TRPM1 (this study). (4) Dialyzing G_{α_o} -GDP is extremely efficient in opening the channel (this study), suggesting that some of the observed effect can be due to direct interaction and not only to sequestering $G\beta\gamma$. While G_{α_o} may be an auxiliary protein, it is unlikely the only one that support channel opening since ON bipolar cells lacking mGluR6 still express G_{α_o} ^{42,46} yet the TRPM1 channels are closed. At least two proteins are required for stable expression of TRPM1 in the membrane, nyctalopin and LRIT3, and in their absence rod bipolar cells are unresponsive to light and the channel is closed or absent from the dendritic tips^{47,48}. Thus it is possible that these two proteins, mGluR6, and/or other unknown components contribute not only to trafficking and stable expression, but also to maintaining open TRPM1 conformations.

Cooperation between G_{α} and $G\beta\gamma$. While the classical view of G-protein function is that upon GTP/GDP exchange, G_{α} -GTP activates its effector, there are several examples where the effector is activated by $G\beta\gamma$ ^{49,50}. Interestingly, most known $G\beta\gamma$ effectors, including adenylyl cyclase, PLC β , and the G-protein-gated inwardly rectifying potassium channel (GIRK), are also effectors for G_{α} ; i.e., G_{α} cooperates with $G\beta\gamma$ to modulate the downstream activity^{51–55}. The GIRK channel provides an especially interesting example because being a channel, the function and interaction of the G-protein subunits with it can readily be compared to their function and interaction with TRPM1. It is well known that GIRK is directly gated by $G\beta\gamma$ ^{56,57}, but the function of $G_{\alpha_{i/o}}$ in the GIRK- $G_{\alpha}\beta\gamma$ complex is emerging more slowly. It is now understood that the non-activated $G_{\alpha_{i3}}$ has 3 independent functions: it reduces the basal current of GIRK, enhances the evoked current, and regulates its kinetics^{58–60}. Both $G_{\alpha_{i3}}$ -GDP and $G_{\alpha_{i3}}$ -GTP interact and regulate GIRK1/2⁶¹. Thus, the analogy of the interaction of the G-protein with the GIRK channel to that with TRPM1 holds on several levels, but the effects of the G-protein subunits are opposite. While $G\beta\gamma$ opens GIRK, it closes TRPM1. While $G_{\alpha_{i/o}}$ -GDP reduces the basal GIRK current, G_{α_o} -GDP seems to increase the basal TRPM1 current. In either case, both G_{α} -GDP and G_{α} -GTP are retained in the complex, and G_{α} -GTP works synergistically with $G\beta\gamma$ ⁶¹. The simplest model that can explain the TRPM1-G-protein interaction (summarized in Fig. 6) is that G_{α_o} -GDP $\beta\gamma$ binds TRPM1 and endows it with an open conformation; when GTP replaces GDP, $G\beta\gamma$ 13 dissociates from G_{α_o} -GTP and both arms twist TRPM1 and change its conformation to the close state. $G\beta\gamma$ binds to TRPM1 probably via its N-terminus, while G_{α_o} may bind both ends of TRPM1. We speculate that G_{α_o} swings from one terminus to the other upon nucleotide exchange; when GDP-bound, it joins $G\beta\gamma$ at the N-terminus, and when GTP-bound, it binds the C-terminus. It is important to remember that the macromolecular complex must contain other proteins as well since G_{α_o} -GDP $\beta\gamma$ must also bind mGluR6 to be activated, and G_{α_o} -GTP must also bind the GAP complex to be deactivated.

Materials and Methods

Ethical approval. Procedures involving animals were performed in accordance with National Institute of Health guidelines and the protocol was reviewed and approved by the Institutional Animal Care and Use Committee of the University of Pennsylvania and the competent ethics committees at Jinan University. C57BL/6J wild type mice (WT) were purchased from Charles River laboratories. A mouse was deeply anesthetized by intraperitoneal injection of a mixture of 100 μ g/gm ketamine and 10 μ g/gm xylazine; the eyes were enucleated and the mouse was euthanized by anesthetic overdose.

Whole cell recording experiments. *Recording.* Retinal slices were prepared as described previously⁶². Briefly, retinas were isolated under red light and cut into 200 μ m thick slices with a tissue slicer (Narishige, Japan). The slices were transferred to a recording chamber, secured with vacuum grease and then moved to the microscope stage of an Olympus microscope equipped with a 60x water immersion objective. The chamber was perfused at a rate of 0.5–1 ml/min with oxygenated (95% O_2 , 5% CO_2) Ames medium (Sigma, St. Louis, MO) containing sodium bicarbonate (1.9 g/l) and 2 μ M Strychnine and 100 μ M picrotoxin (to block GABA_{A/C} receptors) at 32–34°C.

Patch pipettes with resistances of 7–9 M Ω were fabricated from borosilicate glass using an electrode puller (Sutter, Novato, CA). Pipettes were filled with the following solutions (in mM): 108 Cs-gluconate, 10 BAPTA, 10

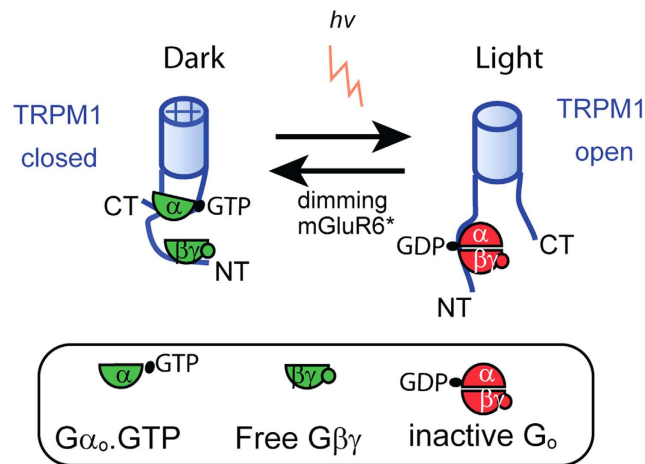


Figure 6. A model for TRPM1 gating. In the dark, mGluR6 is bound to glutamate and G_o is active (depicted in green). Both active G_{α_o} and free $G\beta\gamma$ contribute to channel closure, and both can interact with TRPM1. We speculate that $G\beta\gamma$ is bound to the N-terminus and $G_{\alpha_o}.GTP$ to the C-terminus; both twisting the channel to close it. When light decreases glutamate, and hence deactivates G_o (depicted as red), the heterotrimer G_o is reformed and allows the channel to open. Not shown in the model are other proteins that must interact with this complex to allow these activities to cycle; in particular, mGluR6 must bind the inactive G_o , and the GTPase-activating complex must bind $G_{\alpha_o}.GTP$.

HEPES, 10 NaCl, 4 MgATP and 1 LiGTP. The pH was adjusted to 7.4 with KOH and the osmolality was 290 mOsmol. All chemicals were obtained from Sigma. The solution was aliquoted, stored at $-20\text{ }^{\circ}\text{C}$ and thawed before each experiment. For each set of experiments, we patched several cells with electrodes that contained the above control solution, and several with electrodes that also contained a modifier reagent as explained in Results.

Source of modifier reagents. Myristoylated $G_{\alpha_{o1}}$ (hence referred to as myr G_{α_o}) was obtained from Calbiochem and used for most experiments; myr G_{α_o} -Q205L and its control myr G_{α_o} were prepared as described below; $GTP\gamma S$ was obtained from Sigma (Sigma-Aldrich, St Louis, MO); phosducin was a gift from Dr. Vadim Arshavsky (Duke University); and His₆- G_{α_o} was a gift from Dr. Richard Neubig (University of Michigan).

Current recordings in the US were obtained with an Axopatch 1D amplifier (Molecular Devices) and in China with an EPC-10 patch clamp amplifier (HEKA, Lambrecht, Germany). Membrane potentials were corrected for liquid junction potential calculated to be $\sim 15\text{ mV}$. Cells were discarded if the baseline current in the dark exceeded -100 pA at a holding potential of -60 mV . Voltage command generation and data acquisition were accomplished with Clampex (Molecular Devices) or PatchMaster (HEKA). Cells were voltage clamped at -60 mV and the holding current and light-evoked current responses were compared over time for control and different dialyzed reagents. It has been reported that clamping a cell at $+50\text{ mV}$ may extend the recording time because less calcium-dependent desensitization occurs⁶³. However, in our hands, such clamping did not prove beneficial, and we preferred to make the measurements under more physiologically-relevant voltages.

Light stimuli. The retina was stimulated using a green full-field light generated by a light emitting diode with a peak wavelength of 565 nm (or 500 nm in China). During dark adaptation, the light response was tested with a 10 ms flash ($3.8 \times 10^4\text{ photons}/\mu\text{m}^2/\text{s}$) that was turned on every 35 s. To measure changes in slope conductance, a voltage ramp from -95 mV to $+45\text{ mV}$ was applied every 35 s. During light adaptation, a background illumination with an intensity of $1.1 \times 10^4\text{ photons}/\mu\text{m}^2/\text{s}$ was applied immediately after break-in. To test the OFF response, the light was turned off for 1 or 4 s every 35 s. Slope conductance was measured every 35 s while the light was ON. In some cases another ramp was applied during light OFF.

Analysis. For each cell, the baseline current was calculated every 35 s as the average of current for 0.5 s before light ON for dark-adapted retinas or light OFF for light-adapted retinas. The light response was measured as the peak response to a flash of light (ON response). The slope conductance was measured from the linear range between -95 mV to -65 mV . Waveform analysis of the response was done off-line with Clampfit (Molecular Devices). All data are reported as mean \pm SEM (Standard Error of the Mean). The values of the holding current and conductance at different time points after break-in were compared to those at the first sweep using paired Student's t-test using Excell. Differences were considered significant when $p \leq 0.05$. For p values above 0.01, we report the actual value, and for values below 0.01, we simply state $p < 0.01$.

Expression and purification of the myristoylated forms of rat $G_{\alpha_{o1}}$ and $G_{\alpha_{o1}}$ -Q205L subunits (hence referred to as myr G_{α_o} and myr G_{α_o} -QL). For G_{α_o} bacterial expression vector, the full-length rat $G_{\alpha_{o1}}$ (or $G_{\alpha_{o1}}$ -Q205L mutant) cDNA was fused to a C-terminal His₆ tag and cloned into pET21 (Novagen). pHV738 (a gift from Dr. Richard Kahn, Emory University), a vector which contains the human N-myristoyltransferase 1 (hNMT1) and E. coli methionine aminopeptidase (map) genes, was used to express

the eukaryotic N-myristoylation machinery⁶⁴. To increase N-myristoylation efficiency, the *E. coli* formyl-methionine deformylase (*def*) gene additionally was inserted in pHV738, and the resulting plasmid was called pHV738/*def*. The *E. coli* strain BL21-CodonPlus(DE3)-RIPL (Stratagene) was simultaneously transformed with pET21-G α_o WT/His₆ (or pET21-G α_o -QL/His₆) and pHV738/*def*. The transformed cells were grown in terrific broth (TB) supplemented with ampicillin (50 mg/ml), kanamycin (25 mg/ml), and chloramphenicol (34 mg/ml). Bacteria were inoculated and allowed to grow at 37 °C; when the culture reached OD₆₀₀ of 0.6, the temperature was reduced to 25 °C. At OD₆₀₀ of 0.8, 50 μ M sodium myristate (Sigma # M8005) was added, and 10 min later induction of gene expression was triggered with 1M isopropyl- β -D-thiogalactopyranoside (IPTG) (Invitrogen). Cells were incubated under gentle agitation and harvested 16 hours later by centrifugation. Cell pellets were resuspended and sonicated on ice for 4 min (5 sec on/15 sec off). The crude lysate was clarified by centrifugation and purified (at 4 °C) by chromatography over Ni-NTA. MyrG α_o was eluted with 10 mM EDTA in 50 mM Tris-HCl, pH 7.5. The eluted protein fractions were collected and analyzed by SDS-PAGE. Fractions containing myrG α_o were pooled, concentrated, and further purified on a Superdex 200 column (GE Healthcare). The purity of myrG α_o was confirmed by SDS-PAGE gel analysis. After purification, the biological activity of recombinant G α_o subunits was tested by [³⁵S]GTP γ S binding. On average, 1 mole of myrG α_o bound 0.4–0.6 moles of GTP γ S. N-myristoylation, determined by mass spectrometry, showed 80–85% of the protein to be myristoylated. The protein was stored at –80 °C. Further details about purification and testing of the material will be published elsewhere.

DNA constructs. Plasmids used for co-IP experiments from transfected cells were generated as follows: mouse TRPM1 full-length (NM_001039104.2 transcript variant 2) in pcDNA3.1 was previously described⁶⁵; human G β 3 (NM_002074.4 transcript variant 1) and human G γ 13 (NM_016541.2) in pcDNA3.1 were purchased from cDNA.org (cat# GNB0300000–02 and GNG1300000–02); rat G α_{o1} (NM_017327). Plasmids encoding Bioluminescence Resonance Energy Transfer (BRET) sensors were generated using In-Fusion HD cloning system (Clontech) in pcDNA3.1. As templates, we used plasmids encoding the mouse TRPM1 full-length in pcDNA3.1⁶⁵ and the Nanoluc-encoding plasmid pNL1.1 (Promega). Nanoluc was fused in-frame at the C-terminus of the sequences of TRPM1-NT (aa 1–790; TRPM1-NT-Nluc) or TRPM1-CT (aa 1120–1622; TRPM1-CT-Nluc) in pcDNA3.1. The myristoylation signal was added to the N-terminus of each construct to facilitate membrane localization of respective proteins. BRET sensor constructs Venus155–239-G β 1 (human; NM_002074.4 transcript variant 1. Venus sequence corresponding to aa 156–239 was added in the N terminus of G β 1 separated by the linker sequence GGSGGG), Venus1–155-G γ 2 (human; NM_053064.4 transcript variant 1. Venus sequence corresponding to aa 1–155 was added in the N terminus of G γ 2 separated by the linker sequence GGSGGG) and Venus-G α_{o1} (human; NM_020988.2 transcript variant 1. Venus sequence was inserted in G α_o sequence between aa 91–91 flanked on each side by 4 glycine residues) were provided by N.A. Lambert (Medical College of Georgia, Augusta, GA). All constructs were verified by sequencing.

Co-immunoprecipitation Assays. HEK293T cells were grown in six-well plates and transfected with Lipofectamine LTX (Invitrogen). Transfected plasmids encoded the following constructs (per well): 0.42 μ g G α_o , 0.42 μ g G β 3, 0.42 μ g G γ 13 and 1.25 μ g TRPM1 or 1.25 μ g empty pcDNA3.1 vector. After 24 hours, cells were harvested and lysed by sonication in ice-cold PBS IP buffer (150 mM NaCl, 1% Triton X-100, 5 mM MgCl₂ and Complete protease inhibitor tablets) supplemented with three different compositions (GDP: 0.01 μ M GDP; GDP/AlF₄: 0.01 μ M GDP, 10 mM NaF and 0.02 mM AlCl₃; GTP γ S: 0.01 mM GTP γ S). Lysates were cleared by centrifugation at 14,000 rpm for 10 minutes. The supernatant was incubated with 20 μ l of 50% protein G slurry (GE Healthcare) and 3 μ g sheep anti-TRPM1 antibody on a rocker at room temperature for 1 hour. After three washes with the indicated IP buffer, proteins were eluted from beads with 50 μ l of 2X SDS sample buffer. Proteins retained by the beads were analyzed with SDS-PAGE, followed by Western blotting using HRP conjugated secondary antibodies and an ECL West Pico (Thermo Scientific) detection system. Signals were captured on film and scanned by densitometer.

BRET experiments. HEK293T/17 cells were cultured at 37 °C and 5% CO₂ in DMEM supplemented with 10% fetal bovine serum, MEM non-essential amino acids and 1 mM sodium pyruvate. Cells were plated at a density of 50,000 cells/well in a white 96 well plate with clear bottom (Greiner Bio-One) and transfected using Lipofectamine LTX (Invitrogen) and PLUSTM Reagent (Invitrogen). Cells were co-transfected with a fixed concentration of Nanoluc-fused constructs (donors) and increasing concentrations of Venus-fused constructs (acceptors). Empty vector was used to balance the amount of transfected DNA. Readings were obtained 24 h after transfection, immediately following media exchange to PBS containing 0.5 mM MgCl₂ and 0.1% glucose and Nanoluc substrate (Nano-Glo, Promega) diluted 1:100. Fluorescence (Venus; 535 nm with 30 nm band path width) and luminescence (Nanoluc; 475 nm with 30 nm band path width) emissions were recorded simultaneously in real time with a microplate reader (POLARstar Omega, BMG Labtech) equipped with two photomultiplier tubes. The BRET signal was calculated as the ratio of the light emitted by acceptor over the light emitted by the donor. The ratio of emissions at acceptor and donor wavelengths from donor-only samples has been subtracted. All measurements were performed at room temperature.

References

- Masu, M. *et al.* Specific deficit of the ON response in visual transmission by targeted disruption of the mGluR6 gene. *Cell* **80**, 757–765 (1995).
- Vardi, N. & Morigiwa, K. ON cone bipolar cells in rat express the metabotropic receptor mGluR6. *Visual neuroscience* **14**, 789–794 (1997).
- Vardi, N., Duvoisin, R., Wu, G. & Sterling, P. Localization of mGluR6 to dendrites of ON bipolar cells in primate retina. *The Journal of comparative neurology* **423**, 402–412 (2000).

4. Vardi, N., Matesic, D. F., Manning, D. R., Liebman, P. A. & Sterling, P. Identification of a G-protein in depolarizing rod bipolar cells. *Vis Neurosci* **10**, 473–478 (1993).
5. Nawy, S. The metabotropic receptor mGluR6 may signal through G(o), but not phosphodiesterase, in retinal bipolar cells. *J Neurosci* **19**, 2938–2944 (1999).
6. Dhingra, A. *et al.* The light response of ON bipolar neurons requires G[alpha]o. *The Journal of neuroscience: the official journal of the Society for Neuroscience* **20**, 9053–9058 (2000).
7. Dhingra, A. *et al.* Light response of retinal ON bipolar cells requires a specific splice variant of Galpha(o). *The Journal of neuroscience: the official journal of the Society for Neuroscience* **22**, 4878–4884 (2002).
8. Okawa, H., Pahlberg, J., Rieke, F., Birnbaumer, L. & Sampath, A. P. Coordinated control of sensitivity by two splice variants of Galpha(o) in retinal ON bipolar cells. *J Gen Physiol* **136**, 443–454, doi: 10.1085/jgp.201010477 (2010).
9. Dhingra, A. *et al.* Gbeta3 is required for normal light ON responses and synaptic maintenance. *The Journal of neuroscience: the official journal of the Society for Neuroscience* **32**, 11343–11355, doi: 10.1523/JNEUROSCI.1436-12.2012 (2012).
10. Ramakrishnan, H. *et al.* Differential function of Ggamma13 in rod bipolar and ON cone bipolar cells. *The Journal of physiology* **593**, 1531–1550, doi: 10.1113/jphysiol.2014.281196 (2015).
11. Morgans, C. W. *et al.* TRPM1 is required for the depolarizing light response in retinal ON-bipolar cells. *Proc Natl Acad Sci USA* **106**, 19174–19178, doi: 10.1073/pnas.0908711106 (2009).
12. Koike, C., Numata, T., Ueda, H., Mori, Y. & Furukawa, T. TRPM1: a vertebrate TRP channel responsible for retinal ON bipolar function. *Cell calcium* **48**, 95–101, doi: 10.1016/j.ceca.2010.08.004 (2010).
13. Shen, Y. *et al.* A transient receptor potential-like channel mediates synaptic transmission in rod bipolar cells. *J Neurosci* **29**, 6088–6093, doi: 10.1523/JNEUROSCI.0132-09.2009 (2009).
14. Koike, C. *et al.* TRPM1 is a component of the retinal ON bipolar cell transduction channel in the mGluR6 cascade. *Proc Natl Acad Sci USA* **107**, 332–337, doi: 10.1073/pnas.0912730107 (2010).
15. Audo, I. *et al.* TRPM1 is mutated in patients with autosomal-recessive complete congenital stationary night blindness. *American journal of human genetics* **85**, 720–729 (2009).
16. van Genderen, M. M. *et al.* Mutations in TRPM1 are a common cause of complete congenital stationary night blindness. *American journal of human genetics* **85**, 730–736, doi: 10.1016/j.ajhg.2009.10.012 (2009).
17. Nakamura, M. *et al.* TRPM1 mutations are associated with the complete form of congenital stationary night blindness. *Molecular vision* **16**, 425–437 (2010).
18. Dhingra, A. *et al.* Autoantibodies in melanoma-associated retinopathy target TRPM1 cation channels of retinal ON bipolar cells. *The Journal of neuroscience: the official journal of the Society for Neuroscience* **31**, 3962–3967, doi: 10.1523/JNEUROSCI.6007-10.2011 (2011).
19. Bellone, R. R. *et al.* Differential gene expression of TRPM1, the potential cause of congenital stationary night blindness and coat spotting patterns (LP) in the Appaloosa horse (*Equus caballus*). *Genetics* **179**, 1861–1870, doi: 10.1534/genetics.108.088807 (2008).
20. Duncan, L. M. *et al.* Down-regulation of the novel gene melastatin correlates with potential for melanoma metastasis. *Cancer research* **58**, 1515–1520 (1998).
21. Oancea, E. & Wicks, N. L. TRPM1: new trends for an old TRP. *Advances in experimental medicine and biology* **704**, 135–145, doi: 10.1007/978-94-007-0265-3_7 (2011).
22. Shen, Y., Rampino, M. A., Carroll, R. C. & Nawy, S. G-protein-mediated inhibition of the Trp channel TRPM1 requires the Gbetagamma dimer. *Proceedings of the National Academy of Sciences of the United States of America* **109**, 8752–8757, doi: 10.1073/pnas.1117433109 (2012).
23. Devi, S. *et al.* Metabotropic glutamate receptor 6 signaling enhances TRPM1 calcium channel function and increases melanin content in human melanocytes. *Pigment cell & melanoma research* **26**, 348–356, doi: 10.1111/pcmr.12083 (2013).
24. Nawy, S. & Jahr, C. E. Suppression by glutamate of cGMP-activated conductance in retinal bipolar cells. *Nature* **346**, 269–271, doi: 10.1038/346269a0 (1990).
25. Shiells, R. A. & Falk, G. Glutamate receptors of rod bipolar cells are linked to a cyclic GMP cascade via a G-protein. *Proceedings. Biological sciences / The Royal Society* **242**, 91–94, doi: 10.1098/rspb.1990.0109 (1990).
26. Wong, Y. H. *et al.* Mutant alpha subunits of Gi2 inhibit cyclic AMP accumulation. *Nature* **351**, 63–65, doi: 10.1038/351063a0 (1991).
27. Kroll, S. D. *et al.* The Q205LGo-alpha subunit expressed in NIH-3T3 cells induces transformation. *The Journal of biological chemistry* **267**, 23183–23188 (1992).
28. Higashijima, T., Ferguson, K. M., Sternweis, P. C., Smigel, M. D. & Gilman, A. G. Effects of Mg²⁺ and the beta gamma-subunit complex on the interactions of guanine nucleotides with G proteins. *The Journal of biological chemistry* **262**, 762–766 (1987).
29. Chen, F. & Lee, R. H. Phosducin and betagamma-transducin interaction I: effects of post-translational modifications. *Biochemical and biophysical research communications* **233**, 370–374, doi: 10.1006/bbrc.1997.6460 (1997).
30. Muller, S., Straub, A., Schroder, S., Bauer, P. H. & Lohse, M. J. Interactions of phosducin with defined G protein beta gamma-subunits. *The Journal of biological chemistry* **271**, 11781–11786 (1996).
31. Thulin, C. D. *et al.* Modulation of the G protein regulator phosducin by Ca²⁺/calmodulin-dependent protein kinase II phosphorylation and 14-3-3 protein binding. *The Journal of biological chemistry* **276**, 23805–23815, doi: 10.1074/jbc.M101482200 (2001).
32. Sokolov, M. *et al.* Phosducin facilitates light-driven transducin translocation in rod photoreceptors. Evidence from the phosducin knockout mouse. *The Journal of biological chemistry* **279**, 19149–19156, doi: 10.1074/jbc.M311058200 (2004).
33. Yoshida, T. *et al.* The phosphorylation state of phosducin determines its ability to block transducin subunit interactions and inhibit transducin binding to activated rhodopsin. *The Journal of biological chemistry* **269**, 24050–24057 (1994).
34. Mumby, S. M., Heukeroth, R. O., Gordon, J. I. & Gilman, A. G. G-protein alpha-subunit expression, myristoylation, and membrane association in COS cells. *Proceedings of the National Academy of Sciences of the United States of America* **87**, 728–732 (1990).
35. Venkatachalam, K. & Montell, C. TRP channels. *Annual review of biochemistry* **76**, 387–417, doi: 10.1146/annurev.biochem.75.103004.142819 (2007).
36. Taberner, F. J., Fernandez-Ballester, G., Fernandez-Carvajal, A. & Ferrer-Montiel, A. TRP channels interaction with lipids and its implications in disease. *Biochimica et biophysica acta*, doi: 10.1016/j.bbamem.2015.03.022 (2015).
37. Hille, B., Dickson, E. J., Kruse, M., Vivas, O. & Suh, B. C. Phosphoinositides regulate ion channels. *Biochimica et biophysica acta* **1851**, 844–856, doi: 10.1016/j.bbalip.2014.09.010 (2015).
38. Parnas, M. *et al.* Membrane lipid modulations remove divalent open channel block from TRP-like and NMDA channels. *The Journal of neuroscience: the official journal of the Society for Neuroscience* **29**, 2371–2383, doi: 10.1523/JNEUROSCI.4280-08.2009 (2009).
39. Parnas, M., Peters, M. & Minke, B. Linoleic acid inhibits TRP channels with intrinsic voltage sensitivity: Implications on the mechanism of linoleic acid action. *Channels* **3**, 164–166 (2009).
40. Chyb, S., Raghu, P. & Hardie, R. C. Polyunsaturated fatty acids activate the Drosophila light-sensitive channels TRP and TRPL. *Nature* **397**, 255–259, doi: 10.1038/16703 (1999).
41. Kim, H. *et al.* The roles of G proteins in the activation of TRPC4 and TRPC5 transient receptor potential channels. *Channels* **6**, 333–343, doi: 10.4161/chan.21198 (2012).
42. Xu, Y. *et al.* mGluR6 deletion renders the TRPM1 channel in retina inactive. *Journal of neurophysiology* **107**, 948–957, doi: 10.1152/jn.00933.2011 (2012).
43. Agosto, M. A. *et al.* Oligomeric state of purified transient receptor potential melastatin-1 (TRPM1), a protein essential for dim light vision. *The Journal of biological chemistry* **289**, 27019–27033, doi: 10.1074/jbc.M114.593780 (2014).

44. Schneider, F. M., Mohr, F., Behrendt, M. & Oberwinkler, J. Properties and functions of TRPM1 channels in the dendritic tips of retinal ON-bipolar cells. *European journal of cell biology* **94**, 420–427, doi: 10.1016/j.ejcb.2015.06.005 (2015).
45. Tummala, S. R., Fina, M. E., Dhingra, A. & Vardi, N. G. *Go1* is required for the proper expression of mGluR6 transduction elements in ON-bipolar cells. *ARVO*, Abstract 4314/A4540 (2012).
46. Cao, Y. *et al.* Retina-specific GTPase accelerator RGS11/G beta 5S/R9AP is a constitutive heterotrimer selectively targeted to mGluR6 in ON-bipolar neurons. *The Journal of neuroscience: the official journal of the Society for Neuroscience* **29**, 9301–9313, doi: 10.1523/JNEUROSCI.1367-09.2009 (2009).
47. Pearing, J. N. *et al.* A role for nyctalopin, a small leucine-rich repeat protein, in localizing the TRP melastatin 1 channel to retinal depolarizing bipolar cell dendrites. *The Journal of neuroscience: the official journal of the Society for Neuroscience* **31**, 10060–10066, doi: 10.1523/JNEUROSCI.1014-11.2011 (2011).
48. Gregg, R. G. *et al.* Proper localization and function of *trpm1* depends on *LRIT3* expression in rod depolarizing bipolar cells *Society for Neuroscience abstract*, poster 036 (2014).
49. Dupre, D. J., Robitaille, M., Rebois, R. V. & Hebert, T. E. The role of Gbetagamma subunits in the organization, assembly, and function of GPCR signaling complexes. *Annual review of pharmacology and toxicology* **49**, 31–56, doi: 10.1146/annurev-pharmtox-061008-103038 (2009).
50. Bomsel, M. & Mostov, K. Role of heterotrimeric G proteins in membrane traffic. *Molecular biology of the cell* **3**, 1317–1328 (1992).
51. Oldham, W. M. & Hamm, H. E. Heterotrimeric G protein activation by G-protein-coupled receptors. *Nature reviews. Molecular cell biology* **9**, 60–71, doi: 10.1038/nrm2299 (2008).
52. Milligan, G. & Kostenis, E. Heterotrimeric G-proteins: a short history. *British journal of pharmacology* **147** Suppl 1, S46–55, doi: 10.1038/sj.bjp.0706405 (2006).
53. Ikeda, S. R. Voltage-dependent modulation of N-type calcium channels by G-protein beta gamma subunits. *Nature* **380**, 255–258, doi: 10.1038/380255a0 (1996).
54. Yevenes, G. E. *et al.* Molecular requirements for ethanol differential allosteric modulation of glycine receptors based on selective Gbetagamma modulation. *The Journal of biological chemistry* **285**, 30203–30213, doi: 10.1074/jbc.M110.134676 (2010).
55. Dascal, N. Ion-channel regulation by G proteins. *Trends in endocrinology and metabolism: TEM* **12**, 391–398 (2001).
56. Logothetis, D. E., Kurachi, Y., Galper, J., Neer, E. J. & Clapham, D. E. The beta gamma subunits of GTP-binding proteins activate the muscarinic K⁺ channel in heart. *Nature* **325**, 321–326, doi: 10.1038/325321a0 (1987).
57. Huang, C. L., Slesinger, P. A., Casey, P. J., Jan, Y. N. & Jan, L. Y. Evidence that direct binding of G beta gamma to the GIRK1 G protein-gated inwardly rectifying K⁺ channel is important for channel activation. *Neuron* **15**, 1133–1143 (1995).
58. Peleg, S., Varon, D., Ivanina, T., Dessauer, C. W. & Dascal, N. G(alpha)(i) controls the gating of the G protein-activated K(+) channel, GIRK. *Neuron* **33**, 87–99 (2002).
59. Rubinstein, M. *et al.* Divergent regulation of GIRK1 and GIRK2 subunits of the neuronal G protein gated K⁺ channel by GalphaiGDP and Gbetagamma. *The Journal of physiology* **587**, 3473–3491, doi: 10.1113/jphysiol.2009.173229 (2009).
60. Rusinova, R., Mirshahi, T. & Logothetis, D. E. Specificity of Gbetagamma signaling to Kir3 channels depends on the helical domain of pertussis toxin-sensitive Galpha subunits. *The Journal of biological chemistry* **282**, 34019–34030, doi: 10.1074/jbc.M704928200 (2007).
61. Berlin, S. *et al.* Two distinct aspects of coupling between Galpha(i) protein and G protein-activated K⁺ channel (GIRK) revealed by fluorescently labeled Galpha(i3) protein subunits. *The Journal of biological chemistry* **286**, 33223–33235, doi: 10.1074/jbc.M111.271056 (2011).
62. Xu, Y. *et al.* Retinal ON bipolar cells express a new PCP2 splice variant that accelerates the light response. *J Neurosci* **28**, 8873–8884, doi: 10.1523/JNEUROSCI.0812-08.2008 (2008).
63. Nawy, S. Regulation of the on bipolar cell mGluR6 pathway by Ca²⁺. *The Journal of neuroscience: the official journal of the Society for Neuroscience* **20**, 4471–4479 (2000).
64. Van Valkenburgh, H. A. & Kahn, R. A. Coexpression of proteins with methionine aminopeptidase and/or N-myristoyltransferase in *Escherichia coli* to increase acylation and homogeneity of protein preparations. *Methods in enzymology* **344**, 186–193 (2002).
65. Cao, Y., Posokhova, E. & Martemyanov, K. A. TRPM1 forms complexes with nyctalopin *in vivo* and accumulates in postsynaptic compartment of ON-bipolar neurons in mGluR6-dependent manner. *The Journal of neuroscience: the official journal of the Society for Neuroscience* **31**, 11521–11526, doi: 10.1523/JNEUROSCI.1682-11.2011 (2011).

Acknowledgements

Supported by NIH grant EY11105 (NV), the National Basic Research Program of China (973 Program) 2011CB707501 (YX), National Natural Science Foundation of China 81470656 (YX), Program of Introducing Talents of Discipline to Universities B14036, EY018139 (KAM), and the Intramural Research Program of the NIH (project Z01-ES-101643 (LB)). We thank Vadim Arshavsky (Duke University) for providing phosducin, Richard Neubig (University of Michigan) for providing His6-G α , Nevin Lambert (Medical College of Georgia, Augusta, GA) for providing BRET sensor. Edited by Mirotnik Editing Services.

Author Contributions

Y.X. and N.V. designed physiological experiments; Y.X., N.V. and S.Y. performed and analyzed physiological experiments; C.O., Y.C., C.C., V.P., L.B. and K.M. designed, performed, and analyzed biochemical experiments; Y.X. and N.V. prepared Figures 1–3; Y.C., C.O. and K.M. prepared Figures 4–5; N.V. and L.B. prepared Figure 6; Y.X., N.V., K.M. and L.B. wrote the manuscript. All authors reviewed the manuscript.

Additional Information

Supplementary information accompanies this paper at <http://www.nature.com/srep>

Competing financial interests: The authors declare no competing financial interests.

How to cite this article: Xu, Y. *et al.* The TRPM1 channel in ON-bipolar cells is gated by both the α and the $\beta\gamma$ subunits of the G-protein G $_o$. *Sci. Rep.* **6**, 20940; doi: 10.1038/srep20940 (2016).



This work is licensed under a Creative Commons Attribution 4.0 International License. The images or other third party material in this article are included in the article's Creative Commons license, unless indicated otherwise in the credit line; if the material is not included under the Creative Commons license, users will need to obtain permission from the license holder to reproduce the material. To view a copy of this license, visit <http://creativecommons.org/licenses/by/4.0/>